

# Strategies for the Anchoring of Metal Complexes, Clusters, and Colloids Inside Nanoporous Alumina Membranes\*\*

Pierre Braunstein,<sup>\*,[a]</sup> Hans-Peter Kormann,<sup>[b]</sup> Wolfgang Meyer-Zaika,<sup>[b]</sup> Raphaël Pugin,<sup>[a], [b]</sup> and Günter Schmid<sup>\*,[b]</sup>

**Abstract:** Two complementary strategies are presented for the anchoring of molecular palladium complexes, of cobalt or platinum clusters or of gold colloids inside the nanopores of alumina membranes. The first consists in the one step condensation of an alkoxysilyl functional group carried by the metal complex with the hydroxy groups covering the surface of the membrane pores. Thus, using the short-bite alkoxysilyl-functionalized diphosphane ligands  $(\text{Ph}_2\text{P})_2\text{N}(\text{CH}_2)_3\text{Si}(\text{OMe})_3$  (**1**) and  $(\text{Ph}_2\text{P})_2\text{N}(\text{CH}_2)_4\text{SiMe}_2(\text{OMe})$  (**2**) derived from  $(\text{Ph}_2\text{P})_2\text{NH}$  (dppa) (dppa = bis(diphenylphosphanyl)amine), the palladium complexes  $[\text{Pd}(\text{dmba})\{\kappa^2\text{-}P\text{-}(\text{Ph}_2\text{P})_2\text{N}(\text{CH}_2)_3\text{Si}(\text{OMe})_3\}] \text{Cl}$  (**3**) and  $[\text{Pd}(\text{dmba})\{\kappa^2\text{-}P\text{-}(\text{Ph}_2\text{P})_2\text{N}(\text{CH}_2)_4\text{SiMe}_2(\text{OMe})\}] \text{Cl}$  (**4**) (dmba-H = dimethylbenzylamine), respectively, were tethered to the pore walls. After controlled thermal treatment, confined and highly dispersed palladium nanoparticles were

formed and characterized by transmission electron microscopy (TEM). This method could not be applied to the cobalt cluster  $[\text{Co}_4(\text{CO})_8(\mu\text{-dppa})\{\mu\text{-}P\text{-}(\text{Ph}_2\text{P})_2\text{N}(\text{CH}_2)_4\text{SiMe}_2(\text{OMe})\}]$  (**7**) owing to its too limited solubility. However, its anchoring was achieved by using the second method which consisted of first derivatizing the pore walls with **1** or **2**. The covalent attachment of the diphosphane ligands provides a molecular anchor that allows subsequent reaction with the cluster  $[\text{Co}_4(\text{CO})_{10}(\mu\text{-dppa})]$  **6** to generate anchored **7** and this step was monitored by UV/Vis spectroscopy. In addition, the presence of carbonyl ligands in the cluster provides for the first time a very sensitive spectroscopic probe in the IR region which confirms

both cluster incorporation and the retaining of its molecular nature inside the membrane. The presence of the bridging dppa ligand in **6** provides additional stabilization and accounts for the selectivity of the procedure. Using this method, platinum clusters (diameter ca. 2 nm) and gold colloids (diameter ca. 13 nm) were immobilized after passing their solution through the functionalized membrane pores. The resulting membranes were characterized by TEM which demonstrated the efficiency of the complexation and showed the high dispersion of the metal loading. The successful application of these methods has demonstrated that nanoporous alumina membranes are not only unique supports to incorporate metal complexes, clusters, or colloids but can also be regarded as functional matrices or microreactors, thus opening new fields for applications.

**Keywords:** cluster compounds • cobalt • colloids • membranes • microporosity • palladium

## Introduction

The design of nanomaterials that present size-dependent functions (e. g. quantum size effects) is of considerable current interest.<sup>[1–4]</sup> Confining highly dispersed metals in the

form of atoms, clusters, or colloids in a mesoporous matrix could provide better defined systems (morphology-based control) and prevent coalescence into larger, ill-defined aggregates. There are obvious implications for the fabrication of microelectronic devices<sup>[5]</sup> and for catalytic reactions whose selectivity may be controlled not only by the size and dispersion of the particles but also by the shape of the nanocavity or nanotube viewed as a unique microreactor.<sup>[6]</sup> Numerous recent reports have emphasized the specific magnetic, optical, electrochemical, chemical, and catalytic properties of nanostructures constructed from molecular clusters or colloids.<sup>[7, 8]</sup>

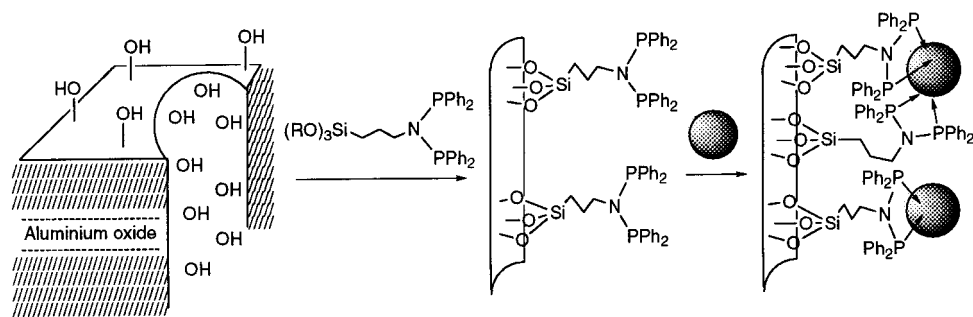
The sol–gel process represents a very efficient method to prepare organic–inorganic hybrid materials from functional building blocks and it has been used to incorporate mono- and bimetallic species into inorganic matrices.<sup>[6c, 8b, 9]</sup> However, morphology control involves both kinetic and thermodynamic

[a] Dr. P. Braunstein, Dipl.-Chem. R. Pugin  
Laboratoire de Chimie de Coordination, UMR 7513 CNRS, Université Louis Pasteur, 4 rue Blaise Pascal  
67070 Strasbourg Cedex (France)  
Fax: (+33)388416030  
E-mail: braunst@chimie.u-strasbg.fr

[b] Prof. Dr. G. Schmid, Dipl.-Chem. H.-P. Kormann,  
Dr. W. Meyer-Zaika, Dipl.-Chem. R. Pugin  
Institut für Anorganische Chemie, Universität Essen  
Universitätsstrasse 5–7, 45117 Essen (Germany)  
Fax: (+49)201-183-2402  
E-mail: guenter.schmid@uni-essen.de

[\*\*] Part of the Doctoral Thesis of R. P. (ULP Strasbourg, June 2000).

**Abstract in French:** Deux stratégies complémentaires ont été élaborées pour l'ancrage de complexes moléculaires de palladium, de clusters de cobalt et ou de platine ainsi que de colloïdes d'or à l'intérieur de membranes d'alumine nanoporeuses. La première d'entre elles consiste à condenser les groupements alkoxy-silyles de complexes métalliques avec les groupements hydroxy recouvrant la surface des membranes d'alumine. De cette manière et à l'aide des ligands assembleurs de type diphosphines fonctionnelles ( $(Ph_2P)_2N(CH_2)_3Si(OMe)_3$  **1** et  $(Ph_2P)_2N(CH_2)_4SiMe_2(OMe)$  **2** dérivant de  $(Ph_2P)_2NH$  (dppa), les complexes de palladium  $[Pd(dmba)\{k^2-P,P-(Ph_2P)_2N(CH_2)_3Si(OMe)_3\}]Cl$  **3** et  $[Pd(dmba)\{k^2-P,P-(Ph_2P)_2N(CH_2)_4SiMe_2(OMe)\}]Cl$  **4** ont été condensés sur les parois des pores. Par la suite, le traitement thermique des membranes contenant les entités moléculaires **3** et **4** condensées donne lieu à la formation de nanoparticules de palladium confinées et hautement monodisperses caractérisées par microscopie électronique à transmission (TEM). Toutefois, cette méthode ne peut être appliquée à la condensation de  $[Co_4(CO)_8(\mu-dppa)\{\mu-P,P-(Ph_2P)_2N(CH_2)_4SiMe_2(OMe)\}]$  **7** en raison de sa faible solubilité. La seconde stratégie adoptée consiste alors à fonctionnaliser tout d'abord la paroi des pores avec **1** ou **2** puis à faire réagir la membrane fonctionnelle avec  $[Co_4(CO)_{10}(\mu-dppa)]$  **6** pour engendrer au sein des pores une espèce moléculaire similaire au cluster **7** condensé. Cette méthode présente en outre l'avantage de pouvoir suivre la complexation de **6** dans la membrane fonctionnalisée par spectroscopie UV-vis. De plus, les ligands carbonyles présents sur le cluster constituent une sonde IR très sensible qui permet de confirmer l'incorporation du cluster ainsi que la rétention de son caractère moléculaire dans la membrane. La présence dans **6** du ligand dppa pontant confère une stabilité accrue qui explique la bonne sélectivité des réactions ultérieures. Cette méthode alternative a de plus permis de complexer, au sein de membranes fonctionnalisées par **1** ou **2**, des clusters de platine (diamètre ca. 2 nm) et des colloïdes d'or (diamètre ca. 13 nm) en passant simplement leur solution respective à travers les pores fonctionnalisés. Ces études ont été suivies par TEM et démontrent l'efficacité de la complexation des nanoparticules ainsi que leur haute dispersion. Par conséquent, ces différentes stratégies démontrent que si les membranes d'alumine nanoporeuses sont d'excellents supports pour incorporer des complexes, clusters et colloïdes, elles peuvent désormais être aussi considérées comme des matrices fonctionnelles ou microréacteurs dans lesquels certaines réactions classiques de chimie de coordination peuvent être menées de manière sélective. De nouvelles perspectives sont dès lors envisageables.



Scheme 1. Functionalization of nanoporous alumina membranes and immobilization of metal clusters or colloids on the pore walls.

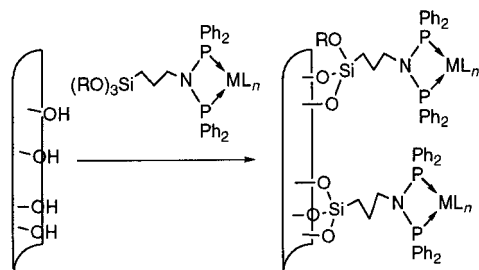
aspects and therefore raises considerable difficulties. On the other hand, the use of solids with a template-based morphology control, such as zeolites and MCM-41, is currently attracting considerable attention.<sup>[6a,b,e,f, 8b, 10]</sup> Well-defined alumina membranes with uniform dimensions and parallel pores can be used as templates for the preparation of gold microtubules, polymeric microcapsules, or nanocomposites of considerable interest, and three- or one-dimensional structures may be generated from colloids or clusters by organizing them in a controlled way.<sup>[11]</sup> Specific advantages of these honeycomblike membranes over other nanoporous materials are the variability of the pore size and pore density as well as the simplicity of producing foils of these materials with sizes up to a few hundred square centimeters.<sup>[12]</sup> By adjusting the anodic voltage used to oxidize the precursor aluminum foil, the pore diameter can be varied between 5 nm and 250 nm, while the pore density decreases from about  $10^{12} \text{ cm}^{-2}$  down to  $10^8 \text{ cm}^{-2}$ . Even porous structures with different pore diameters can be made. In addition to their structural variability, we have found that these membranes are optically transparent in the fingerprint regions of the visible, UV, and infrared spectrum and may be stable up to  $1000^\circ\text{C}$ .<sup>[13, 14]</sup>

The nature of the chemical interactions between the metal clusters or colloids and the nanoporous cavity will play an essential role in determining their organization and confinement inside the pores. It therefore becomes particularly attractive to attempt the functionalization of the interior pore surface to improve the selectivity of these interactions. Such an approach has been reported recently where functional amines or thiols have been condensed with surface OH groups of alumina membranes.<sup>[13, 14]</sup> Our recent findings showing that alkoxy-silyl-substituted short-bite diphosphane ligands, such as  $(Ph_2P)_2N(CH_2)_mSiR_n(OR)_{3-n}$  ( $m = 3$  or  $4$ ;  $n = 0$  or  $2$ ), strongly bind small transition metal clusters,<sup>[15–17]</sup> suggested the use of such ligands to decorate the interior of alumina membranes.

Herein we will show how this can be achieved and demonstrate that gold colloids and platinum clusters may be immobilized by coordination on the pore walls, simply by passing them in solution through the functionalized nanoporous membranes (Scheme 1).

If mononuclear metal complexes were to be immobilized in a similar manner, one would encounter considerable difficulties in characterizing the resulting material as even highest resolution instruments would not “see” the individual metal atoms. Such highly dispersed metal systems in a confined environment would of course be of considerable interest. It therefore became important to develop an alternative strategy that would consist of first synthesizing well-characterized

mononuclear complexes bearing a functional ligand that could be subsequently condensed with the OH groups covering the pore walls. For comparison with the ligand systems shown in Scheme 1 and in order to provide efficient binding of the metal complex, we focused on chelating diphosphane ligands that should make metal leaching much less likely than when monodentate ligands are used (Scheme 2).<sup>[18]</sup>



Scheme 2. Anchoring of a functionalized metal complex on the pore walls of nanoporous alumina membranes.

It remained to be seen whether the condensation step in the pore walls would proceed in a manner similar to that of the uncoordinated ligand in the previous method. In this case, one could maintain in the final nanomaterial a well-defined molecular species. Since this was shown to be successful, we extended this approach to the immobilization of small molecular clusters to cover a wider range of metal nuclearities.

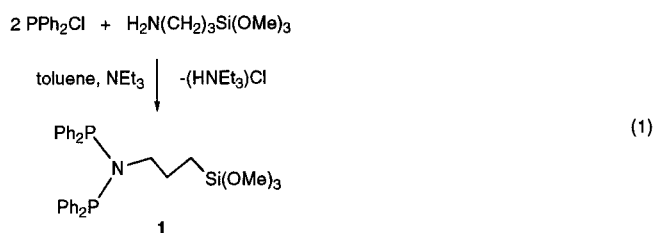
## Results and Discussion

### Derivatization of porous alumina membranes with the alkoxy-silyl-functionalized ligands $(\text{Ph}_2\text{P})_2\text{N}(\text{CH}_2)_3\text{Si}(\text{OMe})_3$ (**1**) and $(\text{Ph}_2\text{P})_2\text{N}(\text{CH}_2)_4\text{SiMe}_2(\text{OMe})$ (**2**): immobilization of metal clusters/colloids in the functionalized porous matrix

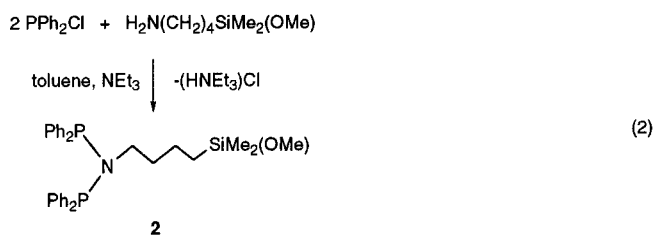
**Synthesis of  $(\text{Ph}_2\text{P})_2\text{N}(\text{CH}_2)_3\text{Si}(\text{OMe})_3$  (**1**) and  $(\text{Ph}_2\text{P})_2\text{N}(\text{CH}_2)_4\text{SiMe}_2(\text{OMe})$  (**2**):** The dppa-type (dppa =  $(\text{Ph}_2\text{P})_2\text{NH}$  = bis(diphenylphosphanyl)amine) backbone of **1** and **2** was chosen because of its known propensity to favor bidentate behavior, thus allowing the stabilization of many organometallic homo- or heteronuclear complexes or clusters.<sup>[15–17, 19–22]</sup> Despite the increased acidity of the NH proton of the dppa ligand upon coordination, functionalization of coordinated dppa by deprotonation and derivatization of the nitrogen atom by an appropriate electrophile cannot always be achieved.<sup>[17]</sup> Therefore, an alternative approach to functionalize clusters was recently designed which consisted of the synthesis of a diphosphane ligand containing a trialkoxysilyl group, followed by its coordination to a metal cluster.<sup>[16]</sup> The first diphosphane ligand used was  $(\text{Ph}_2\text{P})_2\text{N}(\text{CH}_2)_3\text{Si}(\text{OEt})_3$ , which was prepared by reaction of 3-aminopropyltriethoxysilane with two equivalents of  $\text{PPh}_2\text{Cl}$  in the presence of triethylamine.<sup>[15]</sup>

In order to fine-tune the subsequent condensation of such alkoxy-silylphosphane ligands inside nanoporous materials (see below), it was desirable to prepare mono- and trimethoxy analogues of variable chain lengths since it is known that

$\text{Si}(\text{OMe})_3$  groups condense faster than  $\text{Si}(\text{OEt})_3$ . However, if three-dimensional self-condensation of the phosphane ligands occurs, polymers would form that will be difficult or impossible to remove from the desired functionalized nanoporous material. Therefore, we also used a  $\text{SiMe}_2(\text{OMe})$  end-group that could only form dimers upon self-condensation and these should be easier to remove from the porous material. Using a slightly modified method to that reported for  $(\text{Ph}_2\text{P})_2\text{N}(\text{CH}_2)_3\text{Si}(\text{OEt})_3$ ,<sup>[15]</sup> the ligands  $(\text{Ph}_2\text{P})_2\text{N}(\text{CH}_2)_3\text{Si}(\text{OMe})_3$  (**1**) and  $(\text{Ph}_2\text{P})_2\text{N}(\text{CH}_2)_4\text{SiMe}_2(\text{OMe})$  (**2**) were prepared according to Equations (1) and (2). Synthetic details are



given in the Experimental Section. Both compounds were obtained pure and were characterized by IR,  $^1\text{H}$ , and  $^{31}\text{P}\{^1\text{H}\}$  NMR spectroscopic methods. The  $^{31}\text{P}\{^1\text{H}\}$  NMR spectra showed in both cases a singlet at about  $\delta = 62.2$ , at low field compared to the value found for dppa at  $\delta = 43.5$ . A downfield shift of about 20 ppm is typical for a derivatized dppa ligand and is also similar to that observed on going from coordinated dppa to coordinated  $(\text{Ph}_2\text{P})_2\text{NMe}$ .<sup>[17]</sup>



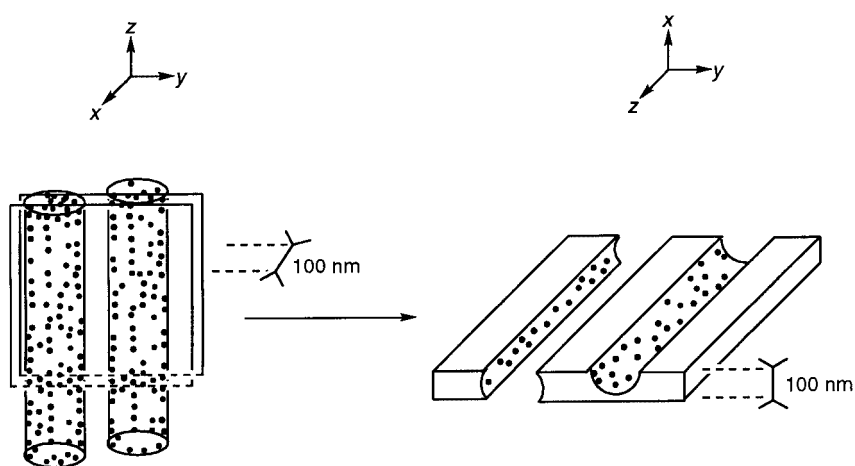
### Derivatization of porous alumina membranes with **1** and **2**: immobilization of clusters/colloids in the modified porous matrix:

Commercially available porous aluminum oxide membranes, Anopore (Merck, Germany, cylindrical pores of 200 nm average diameter) were derivatized with the alkoxy-silyl phosphanes **1** and **2** in order to allow subsequent coordination of gold colloids and platinum clusters (Scheme 1). Condensation of the alkoxy-silyl end-group  $\text{SiMe}_n(\text{OMe})_{3-n}$  of **1** or **2** ( $n = 0$  or  $2$ ) with the highly reactive hydroxy groups covering the alumina surface was performed under reflux conditions. The formation of stable Al-O-Si bonds on the pore walls allows the elimination by rinsing of the remaining uncondensed ligand. After a reaction time of 20 h, the functionalization of the membranes was completed. The anchoring of the functionalized ligands **1** and **2** was confirmed in the IR spectra of the membranes which showed three absorptions at 3058 (w), 2958 (w), and 2930 (w)  $\text{cm}^{-1}$ , close to those observed in  $\text{CH}_2\text{Cl}_2$  for the free ligand, and attributed to the  $\nu_{\text{sym}}(\text{C}-\text{H}, \text{CH arom.})$  and  $\nu(\text{C}-\text{H}, \text{CH}_2)$  stretching vibrations. The characteristic band at 2842  $\text{cm}^{-1}$  for

$\nu_{\text{sym}}(\text{C-H}, \text{Si}(\text{OMe})_{3-n}, n = 0 \text{ or } 2)$  of **1** and **2** was no longer observed, which indicated that unreacted ligand had been completely removed and would not later interfere with the IR fingerprints of the functionalized membrane.

Two different procedures, vacuum filling and impregnation, which are detailed in the Experimental Section, have been used to immobilize gold colloids (diameter ca. 13 nm) or platinum clusters (diameter ca. 2 nm). In both cases, qualitatively similar results were obtained and a dramatic change of the membrane color was first observed. While derivatized alumina membranes are colorless before the incorporation of the metal clusters/colloids, metal-loaded membranes display intense colors (dark red for those containing gold colloids, dark brown in the case of platinum clusters). The metal-loaded Anopore membranes were then embedded in a resin, sectioned parallel to the pore axis into 100 nm thick sheets and submitted to transmission electron microscopy (TEM) investigations. The latter showed the hoped-for presence of immobilized monodisperse particles without any aggregation (Figure 1 and Scheme 3).

These unprecedented results are particularly interesting since efficient immobilization of metal particles in the pores could not be achieved with alkoxysilyl-functionalized *monodentate* phosphanes as ligands, in contrast to the situation on glass or quartz substrates.<sup>[23]</sup> Improvements were observed with membranes derivatized with alkoxysilyl-functionalized primary amines. This was explained by strong acid–base



Scheme 3. View of the particles inside the pores. When two consecutive cuts hit the same pore, only the colloids/clusters immobilized on the walls perpendicular to the (yz) section plane are observed. When the pore has been sectioned only once in the (yz) section plane, colloids/clusters immobilized on the back wall are also observed.

interactions between the amino functions and the citric acid present on the colloid surface.<sup>[13]</sup> In the present study, the driving force for the immobilization of the particles is attributed to the complexing ability of the dppa backbone of **1** and **2** (as chelate or bridge).<sup>[15–17, 19–22]</sup>

#### Tethering of mononuclear Pd complexes [Pd(dmba){ $\kappa^2$ -*P,P*-(Ph<sub>2</sub>P)<sub>2</sub>N(CH<sub>2</sub>)<sub>3</sub>Si(OMe)<sub>3</sub>}Cl (**3**) and [Pd(dmba){ $\kappa^2$ -*P,P*-(Ph<sub>2</sub>P)<sub>2</sub>N(CH<sub>2</sub>)<sub>4</sub>SiMe<sub>2</sub>(OMe)}Cl (**4**) inside porous alumina membranes (dmba-H = dimethylbenzylamine)

Owing to the well-known catalytic properties of Pd complexes in numerous reactions such as hydrogenation of alkenes and alkynes, carbon–carbon coupling reactions, isomerization, etc., the confinement of well-characterized mononuclear palladium complexes in a nanoporous matrix appeared very exciting. In addition to their own properties and reactivity,

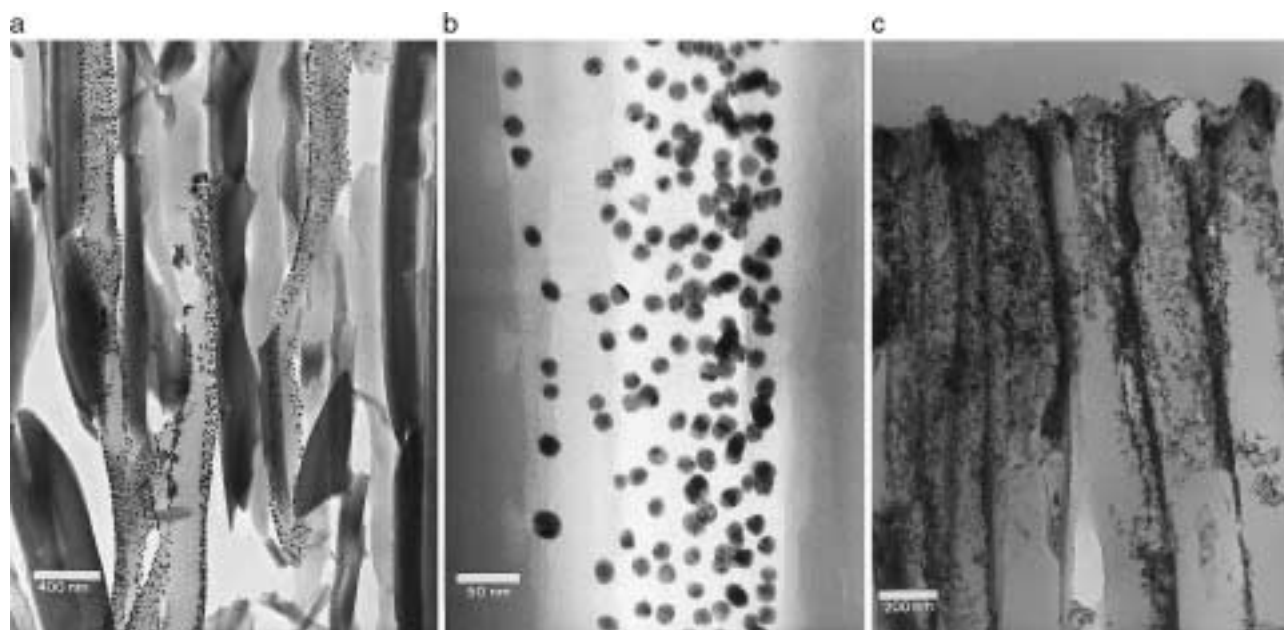
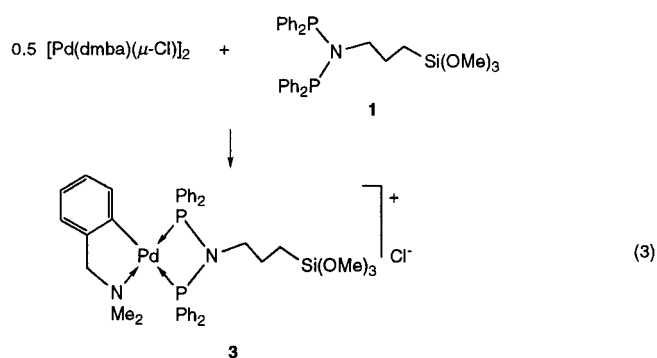


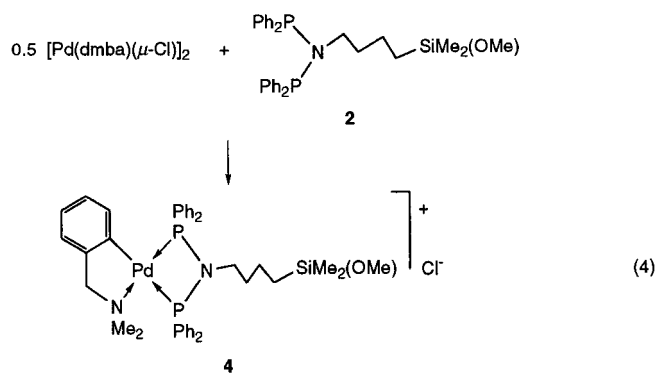
Figure 1. TEM images of gold colloids (a, b; ca. 13 nm) and platinum clusters (c; ca. 2 nm) immobilized with the vacuum-filling method in opened pores of alumina membranes.

these confined and well-dispersed mononuclear complexes could lead after thermal treatment to nanoparticles of narrow size distribution. The preparation of colloidal metals in constrained environments is currently an active area of research. Micelles, vesicles, or zeolite cages have already been used as nanocapsules or microreactors for the preparation and stabilization of confined metal clusters or colloids.<sup>[6f, 24]</sup> Since nanoporous alumina membranes may be stable up to 1000 °C, complexes **3** and **4** (see below) were first tethered and subsequent calcination was performed at various temperatures in order to observe a temperature dependence on the size of the resulting metal particles.

**Synthesis of [Pd(dmba){κ<sup>2</sup>-P,P-(Ph<sub>2</sub>P)<sub>2</sub>N(CH<sub>2</sub>)<sub>3</sub>Si(OMe)<sub>3</sub>}]Cl (3) and [Pd(dmba){κ<sup>2</sup>-P,P-(Ph<sub>2</sub>P)<sub>2</sub>N(CH<sub>2</sub>)<sub>4</sub>SiMe<sub>2</sub>(OMe)}]Cl (4):** When the ligand **1** or **2** was treated with 0.5 equivalents of the dinuclear complex [Pd(dmba)(μ-Cl)]<sub>2</sub> (dmba-H = dimethylbenzylamine) in CH<sub>2</sub>Cl<sub>2</sub>, the mononuclear cationic complexes **3** and **4**, respectively, were obtained in 90% yield and isolated as yellow powders [Eq. (3) and (4)].



The <sup>31</sup>P{<sup>1</sup>H} NMR resonances for the coordinated P atoms of **3** appear at δ = 52.7 and 63.7 (<sup>2</sup>J(P,P) = 58 Hz) and at δ = 53.1 and 64.0 (<sup>2</sup>J(P,P) = 58 Hz) for **4**. By comparison with the values for the uncoordinated ligands (δ = 62.2 for both **1** and **2**), one of the resonances is more shifted upon coordination than the other, as also observed for [Pd(dmba){κ<sup>2</sup>-P,P-dppm}]<sup>+</sup>,<sup>[25a]</sup> or [Pd(dmba){κ<sup>2</sup>-P,P-dppaMe}]<sup>+</sup> (<sup>31</sup>P{<sup>1</sup>H} NMR in acetone: δ = 53.1 and 63.6, <sup>2</sup>J(P,P) = 56 Hz, to be compared with δ = 72 for dppaMe) (dppaMe = (Ph<sub>2</sub>P)<sub>2</sub>NMe).<sup>[25b]</sup> When the reactions were carried out in the presence of TlPF<sub>6</sub>, TlCl precipitated and the same <sup>31</sup>P{<sup>1</sup>H} NMR resonances were observed in addition to that for the PF<sub>6</sub> anion. This confirmed



the displacement of both Cl atoms and thus the coordination of both phosphorous atoms. Consistently, no ν(Pd-Cl) vibration was observed in the far IR spectrum of **3** or **4**. The formation of dinuclear species with bridging diphosphanes **1** or **2** was also ruled out since their <sup>31</sup>P{<sup>1</sup>H} NMR spectrum should correspond to a AA'XX' spin system, which is not consistent with the multiplicity of the signals observed.

**Anchoring of the mononuclear complexes 3, 4 inside porous alumina membranes:** When **3** or **4** was dissolved in benzene, its methoxy groups condensed under reflux with the highly reactive hydroxy groups covering the alumina surface. The functionalization of the membranes was monitored by IR spectroscopy and was complete after a reaction time of 20 h. The anchoring of **3** and **4** was confirmed by the presence of three absorptions at 3060 (w), 2960 (w) and 2930 (w) cm<sup>-1</sup>, close to those observed for uncondensed **3** and **4** in CH<sub>2</sub>Cl<sub>2</sub> and attributed to ν<sub>sym</sub>(C-H, CH arom.) and ν(C-H, CH<sub>2</sub>) stretching vibrations. The band at 2842 cm<sup>-1</sup> for ν<sub>sym</sub>(C-H, Si(OMe)<sub>n=0,2</sub>) characteristic for **3** and **4**, was no longer observed. For the first time, the interior of nanoporous alumina membranes was decorated with well-characterized mononuclear complexes.

This anchoring step was then followed by a thermal treatment and as expected, the formation of metal particles was observed and the results are illustrated in Figure 2. In each case, it was verified by transmission electron microscopy that no metal particle was present before thermal treatment.

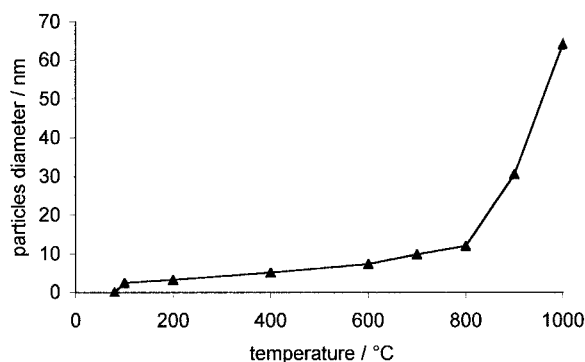
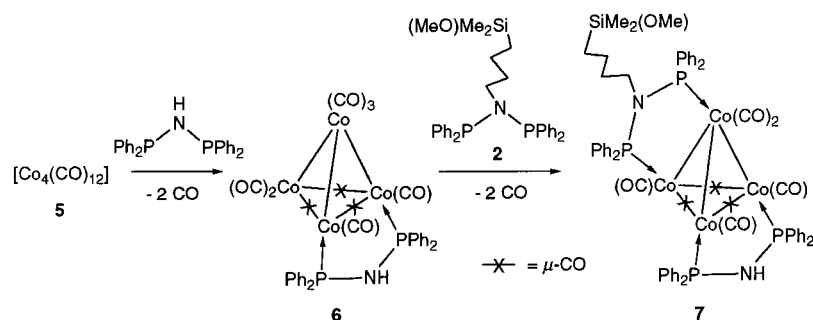


Figure 2. Diameter of confined Pd particles as a function of the activation temperature.

In the temperature range 100–700 °C, the diameter of the particles increased slowly from 2.5 ± 0.5 nm to 9.8 ± 2.0 nm. When the calcination was carried out at temperatures higher than 700 °C, the particle size increased dramatically from 10 nm to reach 64 nm after heating at 1000 °C. These results appear most promising since a wide range of controlled particle sizes becomes available and this will be essential in future comparative investigations of heterogeneous catalytic properties. However, this method did not allow us up to now to fill the pores as densely as achieved above with the platinum clusters and gold colloids. However, varying the parameters such as the average pore diameter, the pore density, or the calcination time should allow identification of the optimum conditions for an increased filling of the pores.

**Tethering of the tetrahedral cluster  $[\text{Co}_4(\text{CO})_8(\mu\text{-dppa})\{\mu\text{-}P\text{-}P\text{-}(\text{Ph}_2\text{P})_2\text{N}(\text{CH}_2)_4\text{SiMe}_2(\text{OMe})\}]$  (**7**) inside porous alumina membranes:** Since we succeeded in tethering mono-nuclear complexes to the alumina surface, while maintaining the well-defined molecular species in the porous structure, we wanted to adapt and extend this strategy to the anchoring of small molecular clusters. We focussed on tetrahedral cobalt carbonyl clusters whose substitution chemistry has shown that the presence of a bridging diphosphane ligand such as dppa greatly increases the stability towards further substitution.<sup>[27a]</sup> Thus,  $[\text{Co}_4(\text{CO})_{10}(\mu\text{-dppa})]$  (**6**) was found to be much more suitable and convenient than  $[\text{Co}_4(\text{CO})_{12}]$  (**5**) for derivatization with the ligand **2**.

**Synthesis and characterizations of  $[\text{Co}_4(\text{CO})_8(\mu\text{-dppa})\{\mu\text{-}P\text{-}P\text{-}(\text{Ph}_2\text{P})_2\text{N}(\text{CH}_2)_4\text{SiMe}_2(\text{OMe})\}]$  (**7**):** The clusters  $[\text{Co}_4(\text{CO})_{12}]$  (**5**)<sup>[26]</sup> and  $[\text{Co}_4(\text{CO})_{10}(\mu\text{-dppa})]$  (**6**)<sup>[21]</sup> were prepared according to the literature and characterized by their IR spectra and, in the case of **6**, also by NMR and UV/Vis spectroscopic methods. The  $^{31}\text{P}\{\text{H}\}$  NMR spectrum of **6** consists of a singlet at  $\delta = 74.2$  ( $\delta = 43.5$  for uncoordinated dppa) consistent with the dppa ligand bridging two equivalent basal cobalt atoms. Cluster **6** was also characterized in UV/Vis spectroscopy by a maximum absorption at about 509 nm. Its reaction with ligand **2** was monitored over 10 h by TLC until all the precursor had reacted to give the mixed ligands cluster  $[\text{Co}_4(\text{CO})_8(\mu\text{-dppa})\{\mu\text{-}P\text{-}P\text{-}(\text{Ph}_2\text{P})_2\text{N}(\text{CH}_2)_4\text{SiMe}_2(\text{OMe})\}]$  (**7**) (Scheme 4).



Scheme 4. Synthetic access to **6** and **7**.

This step required the use of two equivalents of ligand **2** owing to the limited selectivity of the reaction and the formation of by-products, such as  $[\text{Co}_4(\text{CO})_8(\mu\text{-dppa})_2]$  and  $[\text{Co}_4(\text{CO})_8\{\mu\text{-}P\text{-}P\text{-}(\text{Ph}_2\text{P})_2\text{N}(\text{CH}_2)_4\text{SiMe}_2(\text{OMe})\}_2]$  which resulted from ligands redistribution reactions.<sup>[27a]</sup> The product **7** could be separated by chromatography on a silica gel column (see Experimental Section) and obtained pure in 28% yield as a dark brownish green solid. The arrangement of the phosphorus atoms with respect to the metal core of **7** in Scheme 4 is based on that established by X-ray diffraction for related  $\text{Co}_4$  clusters with two bridging diphosphane ligands.<sup>[27b]</sup>

Thus, the  $^{31}\text{P}\{\text{H}\}$  NMR spectrum of **7** shows three resonances at  $\delta = 72.1$  (2P,  $\text{P}_{\text{dppa}} \rightarrow \text{Co}_{\text{basal}}$ ), 92.0 (1P,  $\text{P}_{\text{dppaSi}} \rightarrow \text{Co}_{\text{basal}}$ ), and 103.1 (1P,  $\text{P}_{\text{dppaSi}} \rightarrow \text{Co}_{\text{apical}}$ ) and the  $^1\text{H}$  NMR signals of both P-N-P ligands are present. The IR spectrum of **7** shows two absorptions in the 2010–1970  $\text{cm}^{-1}$  range and three between 1835 and 1760  $\text{cm}^{-1}$ , which are attributed to terminal and bridging carbonyl groups, respectively. Similar

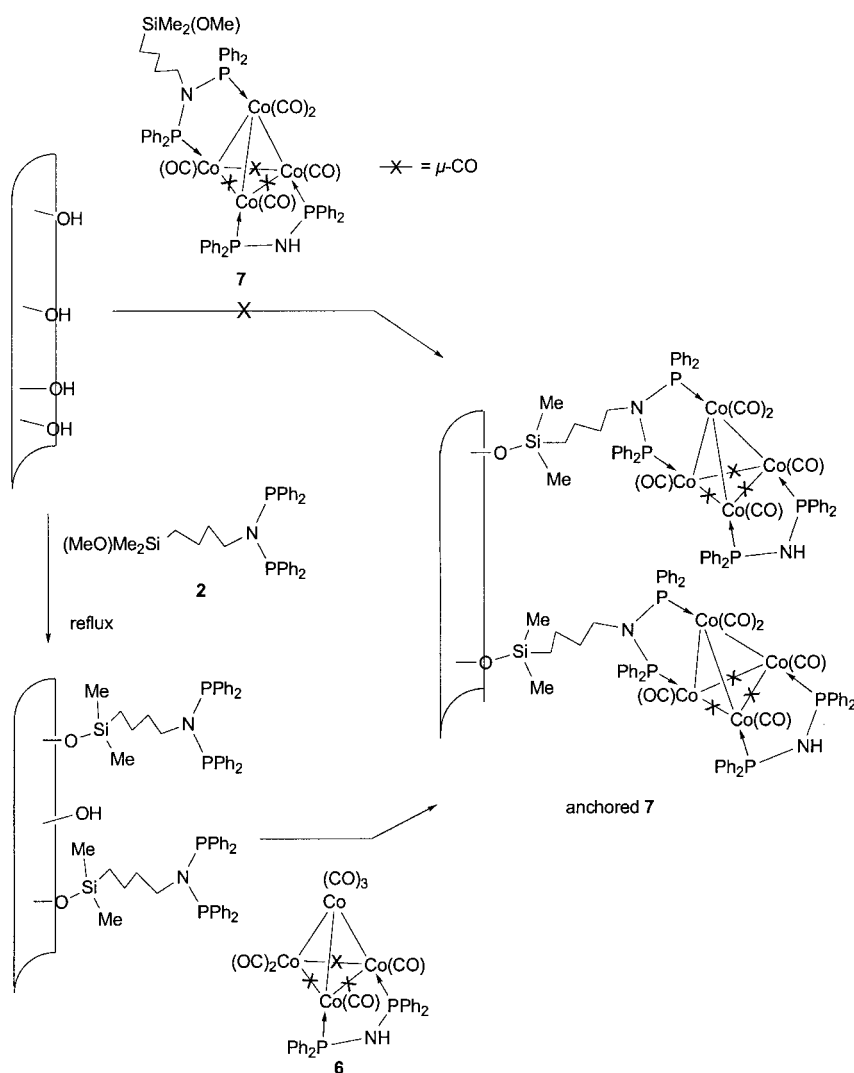
observations were made for  $[\text{Co}_4(\text{CO})_8(\mu\text{-dppa})_2]$  and this pattern appears characteristic of tetrasubstituted  $\text{Co}_4$  tetrahedral derivatives.<sup>[21]</sup> Cluster **7** was also characterized by UV/Vis spectroscopy and presented a maximum absorption at about 614 nm. This wavelength is dramatically shifted when compared to that of **6** (509 nm) and this will turn out to be very useful in the following. Both ligands, dppa and  $(\text{Ph}_2\text{P})_2\text{N}(\text{CH}_2)_4\text{SiMe}_2(\text{OMe})$ , are therefore bridging the cobalt atoms in **7**.

**Anchoring of cluster **7** inside porous alumina membranes:** In order to allow monitoring of the anchoring of the cluster by UV/Vis measurements, transparent nanoporous alumina membranes of high purity (99.99%) with an average pore diameter of 80 nm were prepared since the commercially available porous aluminum oxide membranes (Anopore) were not transparent enough for these measurements. Direct derivatization of the nanoporous alumina membranes with **7** was first attempted. A condensation reaction was expected to take place between the highly reactive hydroxy groups covering the alumina surface and the alkoxy-silyl group of **7** (Scheme 5, top). Unfortunately, this method was unsuccessful and despite the use of different experimental conditions, no detectable membrane functionalization occurred. The membrane remained colorless and IR measurements on treated membranes did not show any absorption characteristic of the cluster. This could be due to the too low solubility of **7**. Thus,

with an estimated total number of OH groups covering the alumina pores of  $1.1 \times 10^{18} \text{ cm}^{-2}$  and even if all the OH groups were condensed with monoalkoxy-silyl-functionalized molecules, only 6.7  $\mu\text{mol}$  of the latter could be anchored on the pore walls.<sup>[28]</sup> Furthermore, considering that membranes always contain water molecules, a large excess of alkoxy-silane functions (empirically found to be 0.25  $\text{mol L}^{-1}$ )

is needed to achieve significant functionalization of the membranes and to characterize them with the available methods. This is much higher than the concentration of a saturated solution of **7** ( $7 \times 10^{-3} \text{ mol L}^{-1}$ ). Moreover the presence of a bulky tetrahedral cobalt cluster could generate steric clutter on the alkoxy-silyl group, thus decreasing also the kinetics of the expected condensation reaction. An alternative explanation for the failure to functionalize the membrane with **7** could be that under the experimental conditions used, a condensation reaction occurred between two molecules of **7** resulting in a dimeric species unable to react further with the OH groups of the membrane.

An alternative and new procedure was then considered in order to achieve indirectly the desired anchoring of **7**. As mentioned above, the reaction between **2** and  $[\text{Co}_4(\text{CO})_{10}(\mu\text{-dppa})]$  (**6**) allowed the synthesis and characterization of **7**. Therefore, it seemed interesting to investigate whether a similar reaction could be carried out inside the pores of the



Scheme 5. Two alternative strategies for the anchoring of clusters onto alumina membranes: (top) unsuccessful direct anchoring of **7** and (bottom) prior functionalization of the alumina membrane with **2** followed by coordination of **6** leading to anchored **7** on the pore walls.

alumina membranes. Nanoporous membranes should then first be functionalized with **2** by the method described above, and then treated with a solution of **6** (Scheme 5, bottom).

In principle, this procedure presents four main advantages. First, due to a higher solubility of **2** compared to **7** in many organic solvents, no concentration problems should occur during membrane functionalization and the resulting nanoporous materials are expected to be highly derivatized. Second, since the molecular approach has shown that the reaction between **2** and **6** took place very rapidly at room temperature, incorporation of the cobalt cluster into the functionalized membranes should require mild conditions, thus avoiding cluster decomposition or dimerization by condensation between SiOMe groups. Third, the dramatic color change observed during the synthesis of **7** (dark brownish green) from **6** (dark red) should help us visualize cluster anchoring on the pores and prove it unequivocally by UV/Vis spectroscopy. Finally, the use of carbonyl clusters should allow monitoring of the anchoring step by IR spectroscopy in the  $\nu(\text{CO})$  region where the membranes are transparent.

This procedure (Scheme 5 (bottom)) was very successful. The functionalization of the membranes with **2** was carried out under reflux and followed by IR spectroscopy (see above). These membranes were then placed in a dark red, concentrated solution of **6**, then washed with  $\text{CH}_2\text{Cl}_2$  in order to remove uncoordinated **6** and finally dried. They presented a dark, brownish green color and showed in UV/Vis spectroscopy a maximum absorption at about 616 nm. By comparison with the electronic spectra of a red solution of **6** or a brownish green solution of **7**, which showed a maximum absorption at about 509 and 614 nm, respectively, this confirmed that the membranes derivatized with **2** had reacted with **6**, thus generating anchored **7** on the pore walls (Figure 3).

The IR spectra of the reacted membranes confirmed these results. The carbonyl bands observed at 2010 (m) and 1977 (s)  $\text{cm}^{-1}$  for cluster-functionalized membranes are directly comparable to those of a solution of **7** at 2009 (m) and 1975 (s)  $\text{cm}^{-1}$  (the carbonyl bands below 1850  $\text{cm}^{-1}$  being no longer observed due to the aluminium oxide absorption in this

spectral region). Moreover, the characteristic carbonyl bands of **6** at 2068 (s), 2030 (s), 2015 (s)  $\text{cm}^{-1}$  were no longer present. Thus, the fact that both the UV/Vis and IR fingerprints of **7**

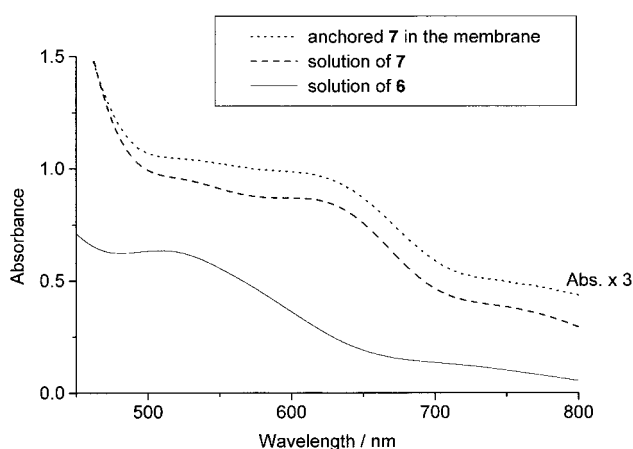


Figure 3. UV/Vis spectra of solutions of **6** and **7** and of the derivatized membrane with anchored **7** on the pore walls.

were clearly recognized in the cluster-functionalized nanoporous membranes unequivocally established the covalent fixation of the  $\text{Co}_4$  cluster in the membrane and the retaining of its molecular nature.

A considerable advantage of this new approach, which consisted of reproducing in nanoporous membranes a molecular coordination chemistry first established on small metal clusters, is its selectivity. In contrast, during the synthesis of **7** from **2** and **6**, by-products were formed and this required tedious purification procedures. Among them,  $[\text{Co}_4(\text{CO})_8(\mu\text{-dppa})_2]$  and  $[\text{Co}_4(\text{CO})_8\{\mu\text{-}P\text{-}P\text{-}(\text{Ph}_2\text{P})_2\text{N}(\text{CH}_2)_4\text{SiMe}_2(\text{OMe})\}_2]$  resulted from facile ligand exchange in solution. Such ligand redistribution reactions should be hindered or suppressed on anchored material and despite the use of a large excess of **2** to functionalize the nanoporous membranes, all the spectroscopic data proved indeed that only one species, anchored **7**, was present in the membrane nanopores. This exciting observation can be easily explained by the fact that in this case the functionalized ligand **2** was chemically strongly attached to the pore walls and could no longer be involved in ligand exchange processes.

## Conclusion

Nanoporous alumina membranes have been shown to represent a convenient matrix to immobilize well-defined inorganic complexes containing functionalized alkoxysilyl-substituted short-bite diphosphane ligands. Their structural versatility as well as their transparency in the fingerprint UV/Vis and IR regions have allowed a precise spectroscopic monitoring of the condensation and anchoring processes of numerous complexes onto the pore walls.

The approach we have developed, which consisted of the synthesis and characterization of mononuclear compounds or small clusters followed by condensation or tethering inside the membranes, offers considerable potential and new perspectives for the use of such porous nanomaterials. The latter provide a constrained environment for the controlled preparation of dispersed metal particles from confined mononuclear complexes.

In contrast to the one-step method which allowed the condensation in nanoporous alumina membranes of alkoxysilyl-functionalized mononuclear complexes such as **3** and **4**, the direct anchoring of **7** could not be achieved. However, an alternative strategy was very successful in which the membranes were first derivatized with the monomethoxysilyl-functionalized P-N-P ligand **2** and then cluster **6** was coordinated on the functionalized pore walls to generate anchored **7** selectively. Therefore, the success of this new alternative method has clearly demonstrated that nanoporous alumina membranes are not only unique supports to incorporate molecular metal clusters, colloids, or metal particles but can also be regarded as functional matrices or microreactors leading to highly selective reactions. This property can therefore open the way to new applications, such as the chemical complexation in membranes of radioactive organometallic compounds for possible clinical use,<sup>[30]</sup> or the possibility for nanoporous membranes to be used as selective

molecular filters. Catalytic studies using membranes containing metal particles are currently in progress and their results will be the subject of future reports.

## Experimental Section

**General considerations:** All reactions with air-sensitive reagents and products were performed under nitrogen using standard Schlenk techniques. All the solvents were dried and purified using standard procedures. NMR spectra were recorded with a Bruker DPX instrument at 300 MHz for  $^1\text{H}$  and 121.5 MHz for  $^{31}\text{P}\{^1\text{H}\}$ . IR spectra of derivatized membranes were recorded on a BIO-RAD FTS-175 infrared spectrometer. Electronic spectra were measured on a Varian Cary-1 UV-Vis spectrometer equipped with a small aperture device. TEM images were obtained by using a Philips FEG-CM 200 instrument working with a 200 kV accelerating voltage. Samples for TEM were embedded in a resin and sectioned. The thickness of the sample was varied from 100 to 50 nm. An Ultra Cut Microtom, Leica, was used for sectioning.

The silanes 3-aminopropyltrimethoxysilane and 4-aminobutyltrimethoxysilane were obtained from Fluka and the complexes  $[\text{Co}_4(\text{CO})_{12}]$ ,<sup>[26]</sup>  $[\text{Co}_4(\text{CO})_{10}(\mu\text{-dppa})]$ ,<sup>[21]</sup> and  $[\text{Pd}(\text{dmba})(\mu\text{-Cl})_2]$ <sup>[31]</sup> were prepared according to the literature methods.

**Synthesis of  $(\text{Ph}_2\text{P})_2\text{N}(\text{CH}_2)_4\text{Si}(\text{OMe})_3$  (**1**):** In a two-neck round-bottomed flask, 3-aminopropyltrimethoxysilane (5.3 mL, 30.0 mmol) and  $\text{NEt}_3$  (9.19 mL, 66.0 mmol) were dissolved in toluene (120 mL). The solution was cooled to  $-40^\circ\text{C}$  and  $\text{Ph}_2\text{P}(\text{Cl})$  (11.14 mL, 60.0 mmol) was added dropwise under vigorous stirring until room temperature was reached and it was stirred for a further 2 h. The solution was then filtered through a cannula, the precipitated ammonium salt was washed several times with toluene/diethyl ether mixtures. The solvent was removed in vacuo ( $25^\circ\text{C}$ , 0.01 Torr) and a slightly yellow oil was obtained. Yield: 14.45 g (88 %); IR ( $\text{CH}_2\text{Cl}_2$ ):  $\tilde{\nu} = 3054\text{ m}$  ( $\nu_{\text{sym}}(\text{C-H arom.})$ ), 2946 m ( $\nu(\text{C-H})$ ,  $\text{CH}_2$ ), 2926 sh ( $\nu(\text{C-H})$ ,  $\text{CH}_2$ ), 2842 m ( $\nu_{\text{sym}}(\text{C-H})$ ,  $\text{Si}(\text{OMe})_3$ ), 1270 s (sym. bending Si-C), 1188 s (rocking  $\text{CH}_3$ ,  $\text{Si}(\text{OMe})_3$ ), 1101  $\text{cm}^{-1}$  vs ( $\nu_{\text{asym}}(\text{Si-O-C})$ )  $\text{cm}^{-1}$ ;  $^1\text{H NMR}$  ( $\text{CDCl}_3$ ):  $\delta = 0.22$  (t, 2H,  $^3J(\text{H,H}) = 8.3$  Hz;  $\text{CH}_2\text{Si}$ ), 1.22 (m, 2H;  $\text{CH}_2\text{-CH}_2\text{Si}$ ), 3.23 (m, 2H;  $\text{CH}_2\text{N}$ ), 3.39 (s, 9H;  $\text{Si}(\text{OMe})_3$ ), 7.25–7.43 (m, 20H;  $\text{PPh}_2$ );  $^{31}\text{P}\{^1\text{H}\}$  NMR ( $\text{CDCl}_3$ ):  $\delta = 62.16$  (s).

**Synthesis of  $(\text{Ph}_2\text{P})_2\text{N}(\text{CH}_2)_4\text{SiMe}_2(\text{OMe})$  (**2**):** In a two-neck round-bottomed flask, 4-aminobutyltrimethoxysilane (1.0 mL, 5.42 mmol) and  $\text{NEt}_3$  (1.66 mL, 11.9 mmol) were dissolved in toluene (25 mL). The solution was cooled to  $-40^\circ\text{C}$  and  $\text{PPh}_2\text{Cl}$  (2.0 mL, 10.85 mmol) was added dropwise under vigorous stirring until room temperature was reached and it was stirred for a further 2 h. The solution was then filtered through a cannula, the precipitated ammonium salt was washed several times with toluene/diethyl ether mixtures. The solvent was removed in vacuo ( $25^\circ\text{C}$ , 0.01 Torr) and a slightly yellow oil was obtained. Yield: 2.58 g (90 %); IR ( $\text{CH}_2\text{Cl}_2$ ):  $\tilde{\nu} = 3054\text{ m}$  ( $\nu_{\text{sym}}(\text{C-H arom.})$ ), 2946 m ( $\nu(\text{C-H})$ ,  $\text{CH}_2$ ), 2926 sh ( $\nu(\text{C-H})$ ,  $\text{CH}_2$ ), 2842 m ( $\nu_{\text{sym}}(\text{C-H})$ ,  $\text{Si}(\text{OMe})_3$ ), 1270 s (sym. bending Si-C), 1188 s (rocking  $\text{CH}_3$ ,  $\text{Si}(\text{OMe})_3$ ), 1101 vs ( $\nu_{\text{asym}}(\text{Si-O-C})$ )  $\text{cm}^{-1}$ ;  $^1\text{H NMR}$  ( $\text{CDCl}_3$ ):  $\delta = -0.04$  (s, 6H;  $\text{Si}(\text{CH}_3)_2$ ), 0.27 (t, 2H,  $^3J(\text{H,H}) = 8.3$  Hz;  $\text{CH}_2\text{Si}$ ), 0.95 (m, 2H;  $\text{CH}_2\text{-CH}_2\text{Si}$ ), 1.11 (m, 2H;  $\text{CH}_2\text{-}(\text{CH}_2)_2\text{Si}$ ), 3.23 (t, 2H;  $\text{CH}_2\text{N}$ ), 3.40 (s, 3H;  $\text{Si}(\text{OMe})_3$ ), 7.18–7.42 (m, 20H;  $\text{PPh}_2$ );  $^{31}\text{P}\{^1\text{H}\}$  NMR ( $\text{CDCl}_3$ ):  $\delta = 62.17$  (s).

**Synthesis of  $[\text{Pd}(\text{dmba})\{\kappa^2\text{-}P\text{-}P\text{-}(\text{Ph}_2\text{P})_2\text{N}(\text{CH}_2)_4\text{Si}(\text{OMe})_3\}]\text{Cl}$  (**3**):** Yellow, solid  $[\text{Pd}(\text{dmba})(\mu\text{-Cl})_2]$  (0.303 g, 0.543 mmol; 0.5 equiv) was added with vigorous stirring to a solution of **1** (0.602 g, 1.086 mmol) dissolved in  $\text{CH}_2\text{Cl}_2$  (75 mL) at  $25^\circ\text{C}$ . The solution was then stirred for 1 h and the solvent was removed in vacuo. The crude product was precipitated by addition of pentane and a yellow solid was collected by filtration. The powder was dried overnight under vacuum. Yield: 0.806 g (90 %); IR ( $\text{CH}_2\text{Cl}_2$ ):  $\tilde{\nu} = 3055\text{ m}$  ( $\nu_{\text{sym}}(\text{C-H arom.})$ ), 2946 m ( $\nu(\text{C-H})$ ,  $\text{CH}_2$ ), 2926 sh ( $\nu(\text{C-H})$ ,  $\text{CH}_2$ ), 2842 m ( $\nu_{\text{sym}}(\text{C-H})$ ,  $\text{Si}(\text{OMe})_3$ ), 1270 s (sym. bending Si-C), 1188 s (rocking  $\text{CH}_3$ ,  $\text{Si}(\text{OMe})_3$ ), 1101 vs ( $\nu_{\text{asym}}(\text{Si-O-C})$ )  $\text{cm}^{-1}$ ;  $^1\text{H NMR}$  ( $\text{CDCl}_3$ ):  $\delta = 0.13$  (t, 2H,  $^3J(\text{H,H}) = 7.7$  Hz;  $\text{CH}_2\text{Si}$ ), 1.10 (m, 2H;  $\text{CH}_2\text{-CH}_2\text{Si}$ ), 2.76–2.86 (m, br., 8H;  $\text{N}(\text{CH}_3)_2$  and  $\text{CH}_2\text{-NP}_2$ ), 3.30 (s, 9H;  $\text{Si}(\text{OMe})_3$ ), 4.14 (s, 2H;  $\text{CH}_2\text{NMe}_2$ ), 6.70–7.09 (m, 4H; phenyl-Pd), 7.59–7.81 (m, 20H;  $\text{PPh}_2$ );  $^{31}\text{P}\{^1\text{H}\}$  NMR ( $\text{CDCl}_3$ ):  $\delta = 52.75$  (d,  $^2J(\text{P,P}) = 58$  Hz), 63.75 (d,  $^2J(\text{P,P}) = 58$  Hz); elemental analysis calcd (%) for



$C_{39}ClH_{47}N_2O_3P_2PdSi$  ( $M_r = 823 \text{ g mol}^{-1}$ ): C 56.92, H 5.71, N 3.40, Pd 12.98; found: C 56.97, H 5.59, N 3.44, Pd 11.95.

**Synthesis of [Pd(dmba)( $\mu$ -Cl)]<sub>2</sub> (**4**):** Solid [[Pd(dmba)( $\mu$ -Cl)]<sub>2</sub>] (0.281 g, 0.508 mmol; 0.5 equiv) was added with vigorous stirring to a solution of **2** (0.538 g, 1.017 mmol) dissolved in  $CH_2Cl_2$  (75 mL) at 25 °C. The solution was then stirred for 1 h and the solvent was removed in vacuo. The crude product was precipitated by addition of pentane and a yellow solid was isolated by filtration. The powder was dried overnight under vacuum. Yield: 0.725 g (88 %); IR ( $CH_2Cl_2$ ):  $\tilde{\nu} = 3056 \text{ m}$  ( $\nu_{\text{sym}}(\text{C-H arom.})$ ), 2946 m ( $\nu(\text{C-H}, \text{CH}_2)$ ), 2926 sh ( $\nu(\text{C-H}, \text{CH}_2)$ ), 2842 m ( $\nu_{\text{sym}}(\text{C-H}, \text{Si}(\text{OMe}))$ ), 1270 s (sym. bending Si-C), 1188 s (rocking  $CH_3$ ,  $Si(\text{OMe})_3$ ), 1101 ( $\nu_{\text{asym}}(\text{Si-O-C})$ )  $\text{cm}^{-1}$ ;  $^1\text{H NMR}$  ( $CDCl_3$ ):  $\delta = -0.05$  (s, 6H;  $Si(\text{CH}_3)_2$ ), 0.14 (t, 2H,  $^3J(\text{H,H}) = 7.7 \text{ Hz}$ ;  $CH_2\text{Si}$ ), 0.85 (m, 2H;  $CH_2\text{-CH}_2\text{Si}$ ), 1.03 (m, 2H;  $CH_2\text{-(CH}_2)_2\text{Si}$ ), 2.77–2.87 (br., 8H;  $N(\text{CH}_3)_2$  and  $CH_2\text{NP}_2$ ), 3.26 (s, 3H;  $Si(\text{OMe})$ ), 4.13 (s, 2H;  $CH_2\text{NMe}_2$ ), 6.70–7.09 (m, 4H; phenyl-Pd), 7.60–7.84 (m, 20H;  $PPh_2$ );  $^{31}\text{P}\{^1\text{H}\}$  NMR ( $CDCl_3$ ):  $\delta = 53.08$  (d,  $^2J(\text{P,P}) = 57 \text{ Hz}$ ), 63.97 (d,  $^2J(\text{P,P}) = 58 \text{ Hz}$ ); elemental analysis calcd (%) for  $C_{40}ClH_{49}N_2O_3P_2PdSi$  ( $M_r = 808 \text{ g mol}^{-1}$ ): C 59.46, H 6.06, N 3.46, Pd 13.17; found: C 59.58, H 6.00, N 3.44, Pd 12.56.

**Synthesis of [Co<sub>4</sub>(CO)<sub>8</sub>( $\mu$ -dppa)]( $\mu$ -P<sub>2</sub>P<sub>2</sub>(Ph<sub>2</sub>P)<sub>2</sub>N(CH<sub>2</sub>)<sub>4</sub>SiMe<sub>2</sub>(OMe)) (7):** Owing to the limited selectivity of this reaction and the formation of several by-products, **2** (2.043 g, 3.863 mmol; two equiv) in  $CH_2Cl_2$  was added at room temperature and under vigorous stirring to a solution of [Co<sub>4</sub>(CO)<sub>10</sub>( $\mu$ -dppa)] (**6**) (1.740 g, 1.932 mmol) in  $CH_2Cl_2$  (100 mL). CO evolution was observed and the reaction was monitored by TLC until all the precursor had reacted (10 h). The solvent was then removed under vacuum. The product could be separated by quantitative chromatography on a 150 mm high silica column ( $\varnothing = 25 \text{ mm}$ , silica gel 60 MERCK, particle size 0.063–0.200 mm). The red cluster **6** (characterized by IR ( $CH_2Cl_2$ )  $\tilde{\nu} = 2068 \text{ s}$ , 2030 s, 2015 s, 1856 w, 1822 m, 1793 ( $\nu(\text{CO})$ )  $\text{m cm}^{-1}$ ;  $R_f = 0.71$  (substance dissolved in  $CH_2Cl_2$ , eluent:  $CH_2Cl_2$ /hexane 60:40)) and green [Co<sub>4</sub>(CO)<sub>8</sub>( $\mu$ -dppa)]<sub>2</sub> were extracted with a mixture  $CH_2Cl_2$ /hexane (40/60). Then, pure **7** was extracted from the column with a mixture  $CH_2Cl_2$ /hexane (60/40) and obtained as a dark brownish green powder. Yield: 0.750 g (0.546 mmol) 28 %; IR ( $CH_2Cl_2$ ):  $\tilde{\nu} = 2009 \text{ s}$ , 1975 s, 1831 w, 1792 m, 1770 ( $\nu(\text{CO})$ )  $\text{m cm}^{-1}$ .  $R_f = 0.13$  (substance dissolved in  $CH_2Cl_2$ , eluent  $CH_2Cl_2$ /hexane 60:40);  $^1\text{H NMR}$  ( $CDCl_3$ ):  $\delta = -0.05$  (s, 6H;  $Si(\text{CH}_3)_2$ ), 0.12 (t, 2H,  $^3J(\text{H,H}) = 7.5 \text{ Hz}$ ;  $CH_2\text{Si}$ ), 0.84 (m, 2H;  $CH_2\text{-CH}_2\text{Si}$ ), 1.10 (m, 2H;  $CH_2\text{-(CH}_2)_2\text{Si}$ ), 2.60–2.80 (br., 2H;  $CH_2\text{NP}_2$ ), 3.25 (s, 3H;  $Si(\text{OMe})$ ), 3.40 (br, 1H; NH), 7.25–7.70 (m, 40H;  $PPh_2$ );  $^{31}\text{P}\{^1\text{H}\}$  NMR ( $CDCl_3$ ):  $\delta = 72.1$  (br, 2P;  $P_{\text{dppa}}\text{-Co}_{\text{basal}}$ ), 92.0 (br, 1P;  $P_{\text{dppaSi}}\text{-Co}_{\text{basal}}$ ), 103.1 (br, 1P;  $P_{\text{dppaSi}}\text{-Co}_{\text{apical}}$ ); elemental analysis calcd (%) for  $C_{63}Co_4H_{58}N_2O_4P_2Si$  ( $M_r = 1374.51 \text{ g mol}^{-1}$ ): C 55.05, H 4.22, N 2.03, Co 17.15; found: C 53.97, H 4.37, N 2.02, Co 16.96.

**Preparation of nanoporous alumina membranes:** Commercially available porous aluminium oxide membrane, Anopore (Merck, Germany; average pore diameter 200 nm) was used for the modification of alumina membranes with functionalized alkoxysilanes in order to coordinate gold colloids and platinum clusters, or for the tethering of mononuclear palladium complexes. The tethering of the cobalt clusters was performed on transparent nanoporous alumina membranes of higher purity (99.99 %) in order to allow UV/vis monitoring and these were prepared according to established procedures.<sup>[11g, 28b]</sup>

**Derivatization of porous alumina membranes with 1–4:** According to well-established procedures to derivatize porous alumina membranes with alkoxysilanes, the membrane was cut in pieces of about  $1 \times 2 \text{ cm}$ , then washed with cyclohexane and dried in an oven at 120 °C. The membrane was then placed in a two-neck round-bottomed flask filled with  $N_2$ . To this flask was added alkoxysilyl-functionalized phosphane **1** or **2** (0.4 mmol) or the mononuclear palladium complexes **3** or **4** (0.4 mmol) dissolved in toluene (20 mL) or benzene, respectively. The solution was heated to reflux temperature overnight without stirring. The solution was then cooled under  $N_2$  atmosphere and the membrane carefully washed with dry toluene or benzene ( $3 \times 10 \text{ mL}$ ) to remove the excess of uncoordinated reagent. The IR spectrum of the newly functionalized membrane was recorded to confirm the functionalization of the pore with the alkoxysilyl-functionalized reagent.

**Immobilization of Au colloids and Pt clusters in functionalized nanoporous alumina membranes:** The unstabilized gold colloid was obtained by reduction of tetrachloroaurate solutions with sodium citrate.<sup>[32]</sup> The

colloidal platinum was obtained by reduction of hexachloroplatinate solutions with sodium citrate.<sup>[33]</sup> The reduction procedure was similar to that described by Turkevich et al.<sup>[34]</sup> To immobilize metal clusters and colloids, two methods were used. The first one consisted in placing the membrane on a short plastic tube connected to a water pump and applying on the other side a drop of the metal cluster/colloid solution. The reduced pressure facilitated transport of the solution through the membrane pores, which resulted in the anchoring of the clusters/colloids to the functionalized walls. The second method consisted of placing the membrane in a round-bottomed flask containing cluster/colloid solution (10 mL) overnight. A static reduced pressure was generated in the flask by use of a water pump. In both cases, the membrane was then washed with water and dried in an oven at 80 °C. This procedure will remove the nanoparticles which would perhaps be inside the pores but not tethered on the pore walls. This immobilization procedure was repeated four times. For both methods, the successful anchoring of the clusters/colloids in the membrane was followed by a dramatic change of the color of this latter. Each sample were then characterized by TEM.

**Complexation of 6 in a porous alumina membrane functionalized with 1 or 2:** The porous alumina membrane was first functionalized with **1** and **2**. By the use of the second anchoring method described above, the functionalized membrane was placed overnight in a red saturated solution of **6** in dry  $CH_2Cl_2$  (8 mL) under a slightly reduced pressure to assist impregnation by capillarity. The membrane was then washed with dry  $CH_2Cl_2$  ( $3 \times 10 \text{ mL}$ ) in order to remove the uncoordinated cluster **6** and dried under vacuum at room temperature. This procedure was repeated four times. The resulting dark brownish green membrane was characterized by different spectroscopic methods such as IR and UV.

## Acknowledgement

The Strasbourg Laboratory is grateful to the CNRS and the Ministère de l'Éducation Nationale, et de la Technologie de la Recherche (Paris) for financial support, and the Essen Laboratory to the European Commission (TMR programme) and the Fonds der Chemischen Industrie.

- [1] U. Simon, G. Schön, G. Schmid, *Angew. Chem.* **1993**, *105*, 264; *Angew. Chem. Int. Ed. Engl.* **1993**, *32*, 250.
- [2] G. Schmid, L. F. Chi, *Adv. Mater.* **1998**, *10*, 515.
- [3] a) G. Schön, U. Simon, *Colloid Polym. Sci.* **1995**, *273*, 101; b) G. Schön, U. Simon, *Colloid Polym. Sci.* **1995**, *273*, 202.
- [4] G. Schmid, *Clusters and Colloids. From Theory to Applications*, Wiley-VCH, Weinheim, **1994**.
- [5] a) U. Simon, *Adv. Mater.* **1998**, *10*, 1487; b) U. Simon in *Metal Clusters in Chemistry, Vol. 3* (Eds.: P. Braunstein, L. A. Oro, P. R. Raithby), Wiley-VCH, Weinheim, **1999**, p. 1342.
- [6] a) B. F. G. Johnson, S. A. Raynor, D. S. Shephard, T. Maschmeyer, J. M. Thomas, G. Sankar, S. Bromley, R. Oldroyd, L. Gladden, M. D. Mantle, *Chem. Commun.* **1999**, 1167; b) R. Raja, G. Sankar, S. Hermans, D. S. Shephard, S. Bromley, J. M. Thomas, B. F. G. Johnson, T. Maschmeyer, *Chem. Commun.* **1999**, 1571; c) E. Lindner, T. Schneller, F. Auer, H. A. Mayer, *Angew. Chem.* **1999**, *111*, 2288; *Angew. Chem. Int. Ed.* **1999**, *38*, 2155; d) P. Braunstein, J. Rosé in *Metal Clusters in Chemistry, Vol. 2* (Eds.: P. Braunstein, L. A. Oro, P. R. Raithby), Wiley-VCH, Weinheim, **1999**, p. 616; e) A. Corma, *Chem. Rev.* **1997**, *97*, 2373; f) S. Kawi, B. C. Gates in *Clusters and Colloid. From Theory to Applications* (Ed.: G. Schmid), Wiley-VCH, Weinheim, **1994**, Chap. 4, p. 298; g) G. A. Ozin, C. Gil, *Chem. Rev.* **1989**, *89*, 1749.
- [7] *Metal Clusters in Chemistry* (Eds.: P. Braunstein, L. A. Oro, P. R. Raithby), Wiley-VCH, Weinheim, **1999**.
- [8] a) N. Toshima, T. Yonezawa, *New J. Chem.* **1998**, *1179*; b) F. Schwyer, P. Braunstein, C. Estournès, J. Guille, H. Kessler, J.-L. Paillaud, J. Rosé, *Chem. Commun.* **2000**, 1271, and references therein.
- [9] a) N. Hüsing, U. Schubert, *Angew. Chem.* **1998**, *110*, 22; *Angew. Chem. Int. Ed.* **1998**, *37*, 22; b) R. J. P. Corriu, D. Leclercq, *Angew. Chem.* **1996**, *108*, 1524; *Angew. Chem. Int. Ed.* **1996**, *35*, 1420; c) P. Braunstein, D. Cauzzi, G. Predieri, A. Tiripicchio, *Chem. Commun.* **1995**, 229; d) P. Braunstein, R. Devenish, P. Gallezot, B. T. Heaton,

- C. J. Humphreys, J. Kervennal, S. Mulley, M. Ries, *Angew. Chem.* **1988**, *100*, 972; *Angew. Chem. Int. Ed.* **1988**, *27*, 927.
- [10] a) J. H. Clark, D. J. Macquarrie, *Chem. Commun.* **1998**, 853; b) J. Y. Ying, C. P. Mehnert, M. S. Wong, *Angew. Chem.* **1999**, *111*, 58; *Angew. Chem. Int. Ed.* **1999**, *38*, 56.
- [11] a) C. R. Martin, *Science*, **1994**, *266*, 1961; b) C. R. Martin, *Adv. Mater.* **1991**, *3*, 457; c) C. R. Martin, R. V. Parthasarathy, *Adv. Mater.* **1995**, *7*, 487; d) S. M. Marinakos, J. P. Novak, L. C. Brousseau III, A. Blaine House, E. M. Edeki, J. C. Feldhaus, D. L. Feldheim, *J. Am. Chem. Soc.* **1999**, *121*, 8518; e) S. M. Marinakos, L. C. Brousseau III, A. Jones, D. L. Feldheim, *Chem. Mater.* **1998**, *10*, 1214; f) H. Masuda, K. Fukuda, *Science*, **1995**, *268*, 1466; g) G. Hornyak, M. Kröll, R. Pugin, T. Sawitowski, G. Schmid, J. O. Bovin, G. Karsson, H. Hofmeister, S. Hopfe, *Chem. Eur. J.* **1997**, *3*, 1951.
- [12] J. P. O'Sullivan, G. C. Wood, "The Morphology and Mechanism of formation of porous anodic films on aluminum", *Proc. Royal Soc. (London)*, **1970**, *317*, 511.
- [13] T. A. Hanaoka, H.-P. Kormann, M. Kröll, T. Sawitowski, G. Schmid, *Eur. J. Inorg. Chem.* **1998**, 807.
- [14] T. A. Hanaoka, A. Heilmann, M. Kröll, H. P. Kormann, T. Sawitowski, G. Schmid, P. Jutzi, A. Klipp, U. Kreibitz, R. Neuendorf, *Appl. Organometal. Chem.* **1998**, *12*, 367.
- [15] I. Bachert, P. Braunstein, R. Hasselbring, *New J. Chem.* **1996**, *20*, 993.
- [16] I. Bachert, P. Braunstein, M. K. McCart, F. Fabrizi de Biani, F. Laschi, P. Zanello, G. Kickelbick, U. Schubert, *J. Organomet. Chem.* **1999**, *573*, 47.
- [17] I. Bachert, I. Bartussek, P. Braunstein, E. Guillon, J. Rosé, G. Kickelbick, *J. Organomet. Chem.* **1999**, *580*, 257.
- [18] D. C. Bailey, S. H. Langer, *Chem. Rev.* **1981**, *81*, 109.
- [19] P. Braunstein, M. Knorr, C. Stern, *Coord. Chem. Rev.* **1998**, *178–180*, 903.
- [20] a) I. Bachert, P. Braunstein, E. Guillon, C. Massera, J. Rosé, A. DeCian, J. Fischer, *J. Cluster Sci.* **1999**, *10*, 445; b) P. Braunstein, J. Durand, G. Kickelbick, M. Knorr, X. Morise, R. Pugin, A. Tiripicchio, F. Ugozzoli, *J. Chem. Soc. Dalton Trans.* **1999**, 4175.
- [21] C. Moreno, M. J. Macazaga, M. L. Marcos, J. Gonzalez-Velasco, S. Delgado, *J. Organomet. Chem.* **1993**, *452*, 185.
- [22] a) J. T. Mague, *J. Cluster Sci.* **1995**, *6*, 217; b) P. Bhattacharyya, J. D. Woollins, *Polyhedron* **1995**, *14*, 3367.
- [23] R. G. Freeman, K. C. Grabar, K. J. Allison, R. M. Bright, J. A. Davis, A. P. Guthrie, M. B. Hommer, M. A. Jackson, P. C. Smith, D. G. Walter, M. J. Natan, *Science*, **1995**, *267*, 1629.
- [24] N. Herron, Y. Wang, H. Eckert, *J. Am. Chem. Soc.* **1990**, *112*, 1322.
- [25] a) J.-F. Ma, Y. Yamamoto, *Inorg. Chim. Acta*, **2000**, *299*, 164; b) J. Blin, P. Braunstein, J. Fischer, G. Kickelbick, M. Knorr, X. Morise, T. Wirth, *J. Chem. Soc. Dalton Trans.* **1999**, 2159, and unpublished results.
- [26] P. Chini, V. Albano, S. Martinengo, *J. Organomet. Chem.* **1969**, *16*, 471.
- [27] a) P. Braunstein, E. Emmrich, J. Rosé, unpublished results; b) H. A. Mirza, J. J. Vittal, R. J. Puddephatt, C. S. Frampton, L. Manojlovic-Muir, W. Xia, R. H. Hill, *Organometallics*, **1993**, *12*, 2767.
- [28] a) We evaluate that for our porous materials, the membrane porosity ( $p$ ) reaches  $5 \times 10^9$  pores  $\text{cm}^{-2}$ .<sup>[28b]</sup> Assuming that the pores are cylindrical, have a 80 nm diameter ( $\varnothing$ ), and that the membrane was 85  $\mu\text{m}$  thick ( $h$ ), the internal surface area of the pores can be calculated as follows:  $S_{\text{int}} = \pi \varnothing h p = 1071 \text{ cm}^2$  for a membrane with an external surface of 1  $\text{cm}^2$ . Considering that the density of hydroxy groups was about 10  $\text{nm}^{-2}$  after treatment at 100 °C,<sup>[29]</sup> the total number of OH groups covering the alumina pores is estimated at  $1.1 \times 10^{18} \text{ cm}^{-2}$ ; b) T. Sawitowski, Ph. D. Thesis, **1999**, Essen, Germany.
- [29] Y. Iwasawa, *Hyoumen*, **1981**, *19*, 161.
- [30] G. Schmid, T. Sawitowski, unpublished results.
- [31] A. C. Cope, E. C. Friedrich, *J. Am. Chem. Soc.* **1968**, *90*, 909.
- [32] G. Schmid, H. Lehnert, *Angew. Chem.* **1989**, *101*, 773; *Angew. Chem. Int. Ed. Engl.* **1989**, *28*, 780.
- [33] P.-A. Brugger, P. Cuendet, M. Grätzel, *J. Am. Chem. Soc.* **1981**, *103*, 2923.
- [34] J. Turckevich, *J. Chem. Phys.* **1945**, *13*, 235.

Received: May 2, 2000 [F2459]